5B.7

NUMERICALLY SIMULATED LIGHTNING PRODUCTION IN SEVERE STORMS

Edward R. Mansell[a,*], **Donald R. MacGorman**[b], **Jerry M. Straka**[c], **Conrad L. Ziegler**[b]

[a]Department of Physics & Astronomy, University of Oklahoma, Norman, OK U.S.A.

[b]National Severe Storms Laboratory, Norman, OK

[c]School of Meteorology University of Oklahoma, Norman, OK

1. INTRODUCTION

Thunderstorm simulations were performed for a strong airmass storm and three types of supercell storms. Several different electrification parameterizations were used for each type of storm. A unique aspect of the simulations was a new, discrete parameterization of lightning discharges. The main focus of our analysis was to examine characteristics of the resulting charge distributions and lightning. Of particular interest are the several supercell storm simulations that produced predominantly positive cloud-to-ground flashes. Results from the airmass storm simulations are also mentioned for comparison.

2. SIMULATION MODEL

The numerical cloud model (Straka and Anderson, 1993) used for the simulations is three dimensional and includes detailed bulk microphysics, with separate categories for cloud water, rain, cloud ice (columns, plates, and rimed), snow aggregates, frozen drops, three graupel densities, and two size ranges of hail. The microphysical package developed by Straka was designed for use on a wide range of circumstances with minimal tuning of parameters. The microphysical parameters were kept constant across all of the simulations.

Each simulation used one of three noninductive charging parameterizations based on laboratory studies of charge separation by rebounding collisions between ice crystals and riming graupel. Noninductive charging is assumed to occur independently of the ambient electric field. The first scheme is based on the Ziegler et al. (1991) adaptation of the Gardiner et al. (1985) parameterization, which was based on the laboratory results of Jayaratne et al. (1983). The Gardiner scheme uses a fixed charge reversal temperature, which was set at $-15°$C for these simulations. Graupel gains negative charge at temperatures lower than the reversal temperature and gains positive charge for collisions occurring at higher temperature. Additionally, the charging is negative at low liquid water content ($< 0.1\,\mathrm{g\,m^{-3}}$) regardless of temperature.

The second noninductive charging scheme is a modified version of the riming rate charging parameterization of Brooks et al. (1997) and Saunders and Peck (1998). In the riming rate scheme, the sign of charge gained by graupel depends on both the ambient temperature and the rime accretion rate of the graupel. The third scheme is a direct implementation of the laboratory results of Takahashi (1978). In the Takahashi scheme, the charge sign is a function of temperature and liquid water content.

Electrification was also allowed by inductive charging (dependent on the electric field) between graupel or hail and rebounding cloud droplets (Ziegler et al. 1991). The effectiveness of the mechanism is varied by changing the average impact angle and separation probabilities, which are kept within the ranges of experimental values. The model also parameterizes the formation of electrical screening layers at cloud boundaries.

Lightning discharges were produced by a stochastic dielectric breakdown model (Wiesmann and Zeller 1986, Mansell 2000) that extends flashes bidirectionally in a step-by-step manner and creates realistic, fractal-like branch structure (Figs. 1 and 2). Discharge channels are propagated step-by-step on a uniform grid with 500 m grid spacing (diagonal directions are allowed). The electric field contribution from the channel charge is computed after each step by solving Poisson's equation ($\nabla^2\phi = -\rho/\epsilon$) for the electric potential ϕ. (The net charge density is ρ, and ϵ is the permittivity of air.) Simulated flashes sometimes deposited enough charge to reverse the local net charge density, and this added complexity to the charge structures of the storms (Fig. 3b,d).

Initiation of flashes occurred whenever the electric field exceeded the so-called 'breakeven' or 'runaway' threshold (Gurevich et al. 1992; Marshall et al. 1995). The breakeven threshold decreases exponentially with increasing altitude and is lower in magnitude than the conventional threshold for air breakdown. In the model, the threshold is at a maximum of 125 kV/m at low altitude and a minimum of 30 kV/m at the top of the domain.

3. STORM ENVIRONMENTS

Three supercell storm environments were utilized which produced a range of supercell storm types, roughly encompassing the range of low precipitation

*Current Affiliation: National Severe Storms Laboratory, 1313 Halley Circle., Norman, OK 73069; *e-mail: mansell@nssl.noaa.gov.*

(LP) to classic (or moderate precipitation) to high precipitation (HP) supercells. A number of experiments were also performed with a low-shear environment (airmass storm). All three supercell environments were characterized by 0–5 km shear magnitudes of about 30 m/s. The HP supercell environment had no shear above 5 km. The LP storm had very strong 5–10 km shear, and the classic supercell had moderately strong 5–10 km shear.

The airmass and HP supercell storms used the same temperature and moisture profiles which are the analytical functions used by Weisman and Klemp (1984). Both storm environments used half-circle hodographs with the wind shear confined to the lowest 5 km, as in Weisman and Klemp (1984). The only difference in the environments of the two storms was the arc length of the hodograph: The airmass storm had a hodograph arc length (U_s) of 10 m/s, whereas the HP supercell storm had $U_s = 50$ m/s. These storms had Convective Available Potential Energy of about 2200 J/kg.

The LP supercell hodograph was constructed by Straka and has slight curvature (veering) in the lowest 5 km. In the 5–10 km layer the shear is nearly linear with a magnitude of about 35 m/s. The temperature profile was the same as for the HP storm, but the moisture was reduced above 3 km altitude.

The classic supercell hodograph had strong curvature (veering) up to 3 km and strong shear through 14 km. It is a composite of two soundings from June 2, 1995, in the Texas panhandle (Gilmore, 2000). The CAPE for the classic storm was about 3000 J/kg.

All the simulations used horizontally homogeneous initial conditions. Each storm was initiated with a warm, moist spheroid of radii $1.5 \times 10 \times 10$ km (12 km for the classic supercell). Vertical grid spacing was fixed at 500 m and horizontal spacing was 1.0–1.5 km, depending on the storm type. The time step was 5.0 s, and runs were carried out to 105 min after initiation.

4. COMPARISON OF CHARGING SCHEMES

The airmass storms all produced $-$CG flashes when the inductive charging was set to be strong, with peak rates of 4–5 min^{-1}. When inductive charging was set to be weaker, however, only the simulation with Takahashi noninductive charging produced any $-$CG lightning. (The simulation with Gardiner noninductive combined with weaker inductive charging produced a single $+$CG.) The inductive charging played an important role in the formation of a lower positive charge region, which was necessary for the initiation of $-$CG lightning flashes.

The Gardiner scheme resulted in the highest charging rates for each of the environments, especially between graupel and snow aggregates. The simulations with Gardiner charging also had the highest IC flash rates. The formulation of the scheme allowed significant negative charging of graupel at relatively low liquid water content, and the strong power-law dependence on crystal size favored larger charge transfer to snow versus ice crystals.

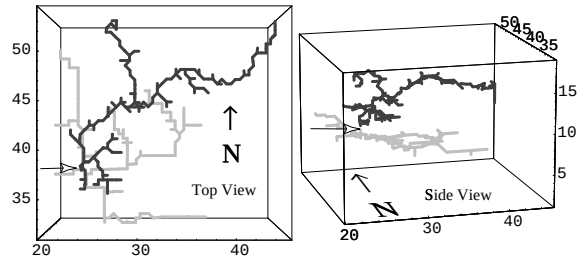

Figure 1: Intracloud flash from a supercell simulation. The positive leaders are shown in gray, the negative leaders in black. Distances are in km, and $\Delta x = \Delta y = \Delta z = 500$ m. The initiation point indicated by the arrow in each view.

The three noninductive charging schemes had distinctly different results in the CG lightning of the three supercell environments. The Gardiner scheme resulted in significant $+$CG lightning (up to 6 min^{-1}) in all three of the supercell types. The Takahashi scheme, on the other hand, produced only $-$CG lightning in the HP and classic supercells and hardly any CG activity in the LP supercell. The LP storm with Takahashi was also by far the lowest producer of IC lightning among the supercell simulations. The riming rate scheme produced a few flashes of both polarities in the HP storm, a number of $+$CG flashes in the classic storm, and fair amounts of both polarities in the LP storm.

A distinguishing characteristic of the Takahashi parameterization not seen in the others was the positive charging of graupel at low liquid water content down to temperatures lower than $-25°$C. This had its greatest effect at the lower cloud boundary of the forward flank and resulted in a layer of positive charge extending out from the positive charge region at the updraft base. This positive layer promoted $-$CG flashes farther away from the surface precipitation regions than with the other noninductive parameterizations.

5. SIMULATED CG LIGHTNING

The majority ($> 90\%$) of lightning discharges in the simulations were intracloud flashes. Currently, a flash is classified as a CG when a leader reaches within 2 km of the ground. (This assumption will be tested in the future.) The polarity of the leader determines the polarity of the CG. Once a flash becomes a CG, the upward-propagating leaders are allowed to continue as for an IC flash, but the downward leaders are halted.

All lightning in the simulations initiated between regions of opposite charge (Fig. 3b,d), where the electric field is strongest, as has been inferred previously for IC flashes and negative cloud-to-ground flashes. However,

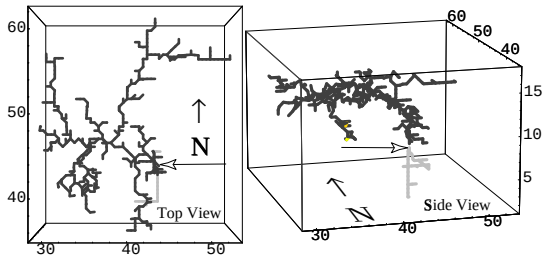

Figure 2: As in Fig. 1 but for a positive cloud-to-ground flash from a supercell simulation.

positive cloud-to-ground flashes also were initiated between opposite charges in our simulations, a relationship not suggested previously. Positive cloud-to-ground lightning in the simulations occurred only when the lowest significant charge region near the initiation point was negative (i.e. roughly a positive dipole structure about the initiation point).

Positive cloud-to-ground lightning (e.g. Fig. 2) occurred predominantly in the supercell storm simulations that used the Gardiner noninductive charging parameterization. The airmass storm simulation with the Gardiner parameterization and strong inductive charging, on the other hand, produced almost exclusively negative CG flashes. As mentioned above, the only environmental difference between the airmass and HP supercell storms was the magnitude of the shear in the 0–5 km layer.

A comparison of the airmass and HP supercell storms with the Gardiner scheme illustrates the differences that led to −CG lightning in the airmass storm and to +CG flashes in the HP supercell. In the airmass case, negatively charged graupel tended to fall through the updraft into high cloud water mixing ratios, where it acquired positive charge via inductive charging. The airmass storm thus developed a strong lower positive charge region which promoted −CG lightning (Fig. 3a-b). In the HP supercell storm (Fig. 3c-d), however, the higher wind shear resulted in more graupel falling outside the updraft, so that a more extended volume of negative graupel developed. The horizontally extensive negative charge resulted in IC and +CG lightning with the positive charge region above (Fig. 3d). Intracloud flashes were regularly initiated between the charge layers in the forward flanks of both storms, but only in the supercell storm did some of those flashes connect to ground to become +CG flashes.

The model result that +CG flashes initiate only between oppositely charged regions (positive above negative) appears to be consistent with the observations reported by Carey and Rutledge (1998). Carey and Rutledge found that a corona point sensor indicated negative charge overhead for regions of a storm that tended to produce positive CG flashes (i.e. the lowest significant charge region was negative). Other observations (e.g. Brook et al. 1982, Fuquay 1982) also have suggested that storms producing +CG flashes have a positive dipole structure (positive charge over negative). However, the commonly mentioned hypotheses to explain the occurrence of +CG flashes all seem to assume that the lowest charge region above the +CG strike point should be positive. The oft-mentioned tilted dipole (or sheared dipole) hypothesis suggests that positive CG flashes might occur if an upper positive charge layer is shifted away from the lower negative charge and becomes "exposed to ground." Likewise, the "inverted dipole" and "enhanced lower positive charge" hypotheses both assume that a lower positive charge causes +CG lightning. The present results suggest that negative charge is needed below positive charge to initiate +CG flashes. However, a flash triggered from ground on a mountain peak or tall structure would presumably access the lowest significant charge (either positive or negative), but this capability is not included in the model.

6. CONCLUSIONS

The results of this research are quite encouraging. The sophisticated cloud microphysics package combined with detailed electrification and lightning parameterizations represent a unique tool for numerical simulations of thunderstorm electrification and lightning. A wide variety of realistic lightning behaviors were successfully produced, including intracloud flashes in the convective and anvil regions and cloud-to-ground flashes of both positive and negative polarities. The intracloud flashes often exhibited a bilevel structure, consistent with many observations. High-altitude intracloud flashes involving an upper negative electrical screening layer occurred in all of the storm simulations. The highest densities of lightning activity in the simulated storms always occurred in the convective regions.

The negative CG flashes produced by the model are consistent with the hypothesis that a lower positive charge region is needed below the main negative region to promote −CG flashes. This hypothesis has been in the literature for many years, though perhaps not widely accepted. The sensitivity tests indicated that inductive charging between graupel and cloud droplets may be important to the development of the lower positive charge. One of the new results of our storm simulations is that a similar hypothesis should apply to positive CG flashes: a *negative* charge region is needed below a positive charge region to promote *positive* CG flashes.

REFERENCES

Brook, M., M. Nakano, P. Krehbiel and T. Takeuti, 1982: The electrical structure of the Hokuriku winter thunderstorms, *J. Geophys. Res.*, **87**, 1207–15.

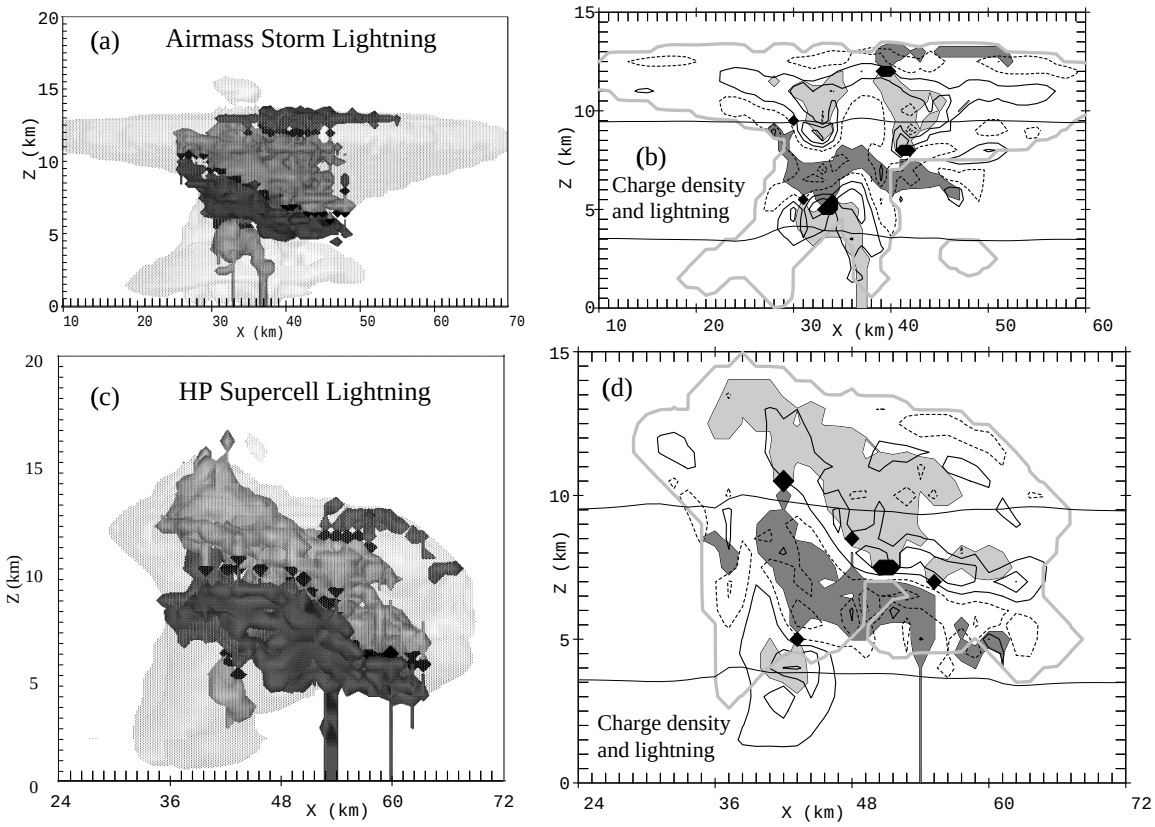

Figure 3: Lightning composites (left) and contour slices (right) for simulations with Gardiner noninductive charging. (a-b) Airmass storm with $-$CG flashes. (c-d) HP supercell with $+$CG flashes. The composites are surfaces over the regions of positive (dark gray) and negative (light gray) lightning leaders during a 2.5 min period. Black surfaces indicate initiation point locations. The slices again show lightning activity regions (light fill for negative leaders, dark for positive, black for initiation locations) overlaid with charge density contours (solid for positive, dashed for negative). Contour values start at $\pm 0.25\,\mathrm{nC\,m^{-3}}$ with intervals of 0.5. Cloud boundary indicated by lightest gray surface (left) or thick gray line (right).

Brooks, I. M. and C. P. R. Saunders, 1995: Thunderstorm charging: laboratory experiments clarified. *Atmos. Res.*, **39**, 263–273.

Carey, L. D. and S. A. Rutledge, 1998: Electrical and multiparameter radar observations of a severe hailstorm. *J. Geophys. Res.*, **103**, 13979–14000.

Fuquay, D. M., 1982: Positive cloud-to-ground lightning in summer thunderstorms. *J. Geophys. Res.*, **87**, 7131–40.

Gardiner, B., D. Lamb, R. L. Pitter, J. Hallett, C. P. R. Saunders, 1985: Measurements of initial potential gradient and particle charges in a montana summer thunderstorm. *J. Geophys. Res.*, **90**, 6079–6086.

Gilmore, M. S., 2000: *Observed and Simulated 2–3 June 1995 West Texas Panhandle Supercells*. Ph.D. diss., Texas A & M, 250 pp.

Gurevich, A. V., G. M. Milikh, and R. Roussel-Dupre, 1992: Runaway electron mechanism of air breakdown and preconditioning during a thunderstorm. *Phys. Lett. A*, **165**, 463–468.

Jayaratne, E. R., C. P. R. Saunders, and J. Hallett, 1983: Laboratory studies of the charging of soft hail during ice crystal interactions. *Q. J. R. Meteorol. Soc.*, **109**, 609–630.

Mansell, E. R., 2000: *Electrification and Lightning in Simulated Supercell and Non-supercell Thunderstorms*. Ph.D. diss., Univ. Oklahoma, 211 pp.

Marshall, T. C., W. D. Rust, W. P. Winn, and K. E. Gilbert, 1989: Electrical structure in two thunderstorm anvil clouds. *J. Geophys. Res.*, **94**, 2171–2181.

Marshall, T. C., M. P. McCarthy, and W. D. Rust, 1995: Electric field magnitudes and lightning initiation in thunderstorms. *J. Geophys. Res.*, **100**, n. D4, 7097–7103.

Saunders, C. P. R., and S. L. Peck, 1998: Laboratory studies of the influence of the rime accretion rate on charge transfer during crystal/graupel collisions. *J. Geophys. Res.*, **103**, 13949–13956.

Straka, J. M. and J. R. Anderson, 1993: Numerical simulations of microburst-producing storms: Some results from storms observed during COHMEX. *J. Atmos. Sci.*, **50**, 1329–1348.

Takahashi, T., 1978: Riming electrification as a charge generation mechanism in thunderstorms. *J. Atmos. Sci.*, **35**, 1536–1548.

Weisman, M. L. and J. B. Klemp, 1984: The structure and classification of numerically simulated convective storms in directionally varying wind shears. *Mon. Weath. Rev.*, **112**, 2479–2498.

Wiesmann, H. J. and H. R. Zeller, 1986: A fractal model of dielectric breakdown and prebreakdown in solid dielectrics. *J. Appl. Phys.*, **60**, 1770–1773.

Williams, E. R., 1989: The tripole structure of thunderstorms. *J. Geophys. Res.*, **94**, 13151–13167.

Ziegler, C. L., D. R. MacGorman, J. E. Dye, and P. S. Ray, 1991: A model evaluation of non-inductive graupel-ice charging in the early electrification of a mountain thunderstorm. *J. Geophys. Res.*, **96**, 12833–12855.